Synthesis of Soluble Phosphate Polymers by RAFT and Their in Vitro Mineralization.

Shuko Suzuki,[†,‡] Michael R. Whittaker,[§] Lisbeth Grøndahl,[*,‡] Michael J. Monteiro,[*,‡,§] and Edeline Wentrup-Byrne[*,†]

Tissue Repair and Regeneration Program, School of Physical and Chemical Sciences, Queensland University of Technology, Brisbane QLD 4001, Australia, School of Molecular and Microbial Sciences, University of Queensland, Brisbane QLD 4072, Australia, and Australian Institute of Bioengineering and Nanotechnology, School of Molecular and Microbial Sciences, University of Queensland, Brisbane QLD 4072, Australia

Received June 18, 2006; Revised Manuscript Received August 23, 2006

Soluble linear (non-cross-linked) poly(monoacryloxyethyl phosphate) (PMAEP) and poly(2-(methacryloyloxy)-ethyl phosphate) (PMOEP) were successfully synthesized through reversible addition−fragmentation chain transfer (RAFT)-mediated polymerization and by keeping the molecular weight below 20 K. Above this molecular weight, insoluble (cross-linked) polymers were observed, postulated to be due to residual diene (cross-linkable) monomers formed during purification of the monomers, MOEP and MAEP. Block copolymers consisting of PMAEP or PMOEP and poly(2-(acetoacetoxy)ethyl methacrylate) (PAAEMA) were successfully prepared and were immobilized on aminated slides. Simulated body fluid studies revealed that calcium phosphate (CaP) minerals formed on both the soluble polymers and the cross-linked gels were very similar. Both the PMAEP polymers and the PMOEP gel showed a CaP layer most probably brushite or monetite based on the Ca/P ratios. A secondary CaP mineral growth with a typical hydroxyapatite (HAP) globular morphology was found on the PMOEP gel. The soluble PMOEP film formed carbonated HAP according to Fourier transform infrared (FTIR) spectroscopy. Block copolymers attached to aminated slides showed only patchy mineralization, possibly due to the ionic interaction of negatively charged phosphate groups and protonated amines.

Introduction

Phosphorus-containing polymers have elicited much interest over several decades because of their usefulness in a wide range of applications such as flame-retardants, ion-exchange resins, dental adhesives, adhesion promoters on metal substrates, and more recently in biomedical applications. One approach to incorporating the phosphorus functionality is through the phosphorylation of polymers. One such example is the reaction of hydroxyl-functionalized polymers with phosphonated epoxide.[1] Alternatively, phosphorus-containing monomers can be polymerized or copolymerized. Among these, the commercially available phosphate-containing monomers monoacryloxyethyl phosphate (MAEP) and 2-(methacryloyloxy)ethyl phosphate (MOEP) have been increasingly studied because of their potential use in various biomedical applications (monomer structures in Scheme 1).[2−6]

Both the homo- and copolymerization of phosphate monomers has previously been found to lead to the formation of insoluble cross-linked networks in conventional free radical polymerization systems. This has been ascribed either to the presence of phosphate diene impurities (in situ cross-linker formed through transesterification) or to excessive chain transfer to the polymer.[7,8] Diene impurities are formed during purification of the monomers by distillation, and even spurious amounts are known to cause cross-linking. MOEP has been copolymerized with various hydrophilic monomers, such as *N*-dimethylacrylamide (DMAA), acrylic acid (AA), hydroxyethyl methacrylate (HEMA), *N*-isopropylacrylamide (NIPAAm), and *N*,*N*′-methylene-bisacrylamide, to produce cross-linked hydrogels which have been shown to have interesting properties with respect to swelling[9,10] and thermosensitivity,[9] as well as being capable of loading cationic biomolecules such as lysozyme.[11] The use of phosphate-containing polymers for the repair and regeneration of bone and cartilage is an approach being used by several research groups. Block copolymers of MOEP and 1-vinyl 2-pyrrolidone or diethylamino ethyl methacrylate have been prepared for bone substitute applications.[4] A more recent study has demonstrated that poly(ethylene glycol) (PEG) hydrogels containing MOEP improved adhesion and spreading of human mesenchymal stem cells.[3]

A series of studies has been concerned with the functionalization of polymer scaffolds and materials with phosphate groups to produce surfaces capable of initiating the cascade of events that lead to calcium phosphate (CaP) mineral nucleation and subsequent biomineralization.[12] Mineralization is a complicated process which, although extensively studied over the years by researchers from diverse disciplines, is still not completely understood. In a series of elegant experiments, Kamei et al.[13] have demonstrated the enhanced bone-bonding ability of MOEP graft copolymers of PE and PET in vivo by implantation in the rat femur. In our earlier studies on MAEP- and MOEP-grafted ePTFE membranes, depending on the monomer and graft copolymer, different mineral phases of CaP were formed.[14,15] Since the ePTFE membrane itself does not induce mineralization, the formation of various CaP phases on these grafted

* Authors to whom correspondence should be sent. E-mail: m.monteiro@uq.edu.au (M.J.M.); e.wentrupbyrne@qut.edu.au (E.W.-B.); grondahl@uq.edu.au (L.G.).

† Queensland University of Technology.

‡ School of Molecular and Microbial Sciences, University of Queensland.

§ Australian Institute of Bioengineering and Nanotechnology.

10.1021/bm060583q CCC: $33.50
Published on Web 10/17/2006

Scheme 1

Monomers

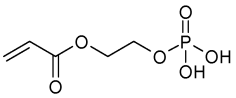

Monoacryloxyethyl phosphate (MAEP) (1)

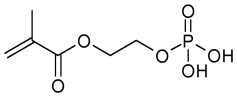

2-(methacryloyloxy)ethyl phosphate (MOEP) (2)

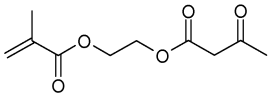

2-(acetoacetoxy) ethyl methacrylate (AAEMA) (3)

RAFT agents

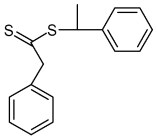

1-Pheylethyl phenyldithioacetate (1-PEPDA) (4)

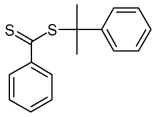

Cumyl dithiobenzoate (CDB) (5)

samples can be attributed solely to the PMAEP or PMOEP moieties. It is, however, difficult to fully characterize the tethered moieties, hence, our target of synthesizing well-defined linear polymers in order to study their mineralization in vitro.

"Living" radical polymerization is the method of choice that enables us to engineer well-defined polymers with tuneable structures, compositions, and properties.[16] Several studies have shown successful "living" radical polymerization of phosphorus-containing monomers. Atom transfer radical polymerization (ATRP) of phosphate-containing monomers in their non-acidic forms such as dimethyl(1-ethoxycarbonyl)vinyl phosphate and deprotonated MOEP have been successfully carried out.[17,18] However, the limited monomer conversion observed suggested that complexation between the copper ions and the phosphoryl oxygen of the phosphonate groups was occurring. 2-Methacryloyloxyethyl phosphorylcholine was polymerized by both the ATRP[19] and reversible addition fragmentation chain transfer (RAFT)[20,21] processes. Phosphonated methacrylates have been successfully copolymerized with vinyldene chloride and methyl acrylate using the RAFT technique.[1] To the best of our knowledge, there are no literature reports for the RAFT polymerization of either MAEP or MOEP.

In this study, we report the first soluble (non-cross-linked) homopolymers of MAEP and MOEP synthesized by RAFT techniques using two different RAFT agents: 1-phenylethyl phenyldithioacetate (1-PEPDA) and cumyl dithiobenzoate (CDB) (Scheme 1). The polymerization reaction was followed by FT-Raman spectroscopy, and the polymers were characterized by gel permeation chromatography (GPC) and microanalysis. In addition, we have prepared block copolymers of MAEP or MOEP and 2-(acetoacetoxy) ethyl methacrylate (AAEMA). The calcification behavior of these polymers using the simulated body fluid (SBF) method[22] was investigated in two ways: either cast films or block copolymers attached to aminated glass slides. Scanning electron microscopy (SEM) coupled with energy-dispersive X-ray spectroscopy (EDS) and Fourier transform infrared (FTIR) spectroscopy were used to characterize the minerals formed. The results were compared to those of the cross-linked polymers to determine the effects of polymer structure on calcification.

Experimental Section

Materials. MOEP was purchased from Aldrich, and the inhibitor was removed by toluene extraction.[4] Inhibitor-free MAEP (Polysciences, 97%) was used as received. AAEMA (Aldrich, 95%) was purified by vacuum distillation. 1-PEPDA and CDB were synthesized and characterized using the method reported elsewhere.[23,24] 2,2-Azobis(isobutyronitrile) (AIBN, Aldrich, 99%) was recrystallized from methanol prior to use. The methanol and ethyl acetate were analytical grade and used as received. The purities of the chemicals used to prepare the SBF solution were as follows: NaCl (99.9%), $NaHCO_3$ (99.0%), Na_2CO_3 (99.9%), KCl (99.0%), K_2HPO_4 (99.0%), $MgCl_2 \cdot 6H_2O$ (99.0%), $CaCl_2 \cdot 2H_2O$ (99.5%), $NaSO_4$ (99.0%), and HEPES (2-[4-(2-hydroxyethyl)-1-piperazinyl]ethanesulfonic acid) (99.9%). Benzoylated dialysis tubing (MwCO 1200) was purchased from Aldrich.

Methods. *Preparation of Homopolymers.* Solutions containing monomer, RAFT agent, and AIBN in methanol were prepared in the concentrations given in Table 1. For example, 2 g of MAEP (1.01 M), 27.2 mg of 1-PEPDA (1×10^{-2} M), and 3.3 mg of AIBN (2×10^{-3} M) were dissolved in 6.7 g of methanol. Aliquots of 1.5 mL were transferred to five individual ampules which were degassed by four freeze−evacuate−thaw cycles and sealed. These samples were placed in an oil bath at 60 °C and removed after the required time such that five different time points were reached for each experiment. Conversion was measured by Raman spectroscopy. The reaction was stopped by cooling the solution in liquid N_2. Soluble polymer samples were purified by dialyzing against methanol for 3 days. Gels were extensively washed with methanol followed by acetone. The samples were dried in a vacuum oven at 40 °C for 2−3 days.

PAAEMA homopolymer was prepared with CDB as a RAFT agent (expt 10 in Table 2). Solutions containing monomer (2.92 M), CDB (0.125 M), and AIBN (0.017 M) in ethyl acetate were prepared. Polymerization was carried out as described previously. Polymerization was stopped after 16.7 h. The polymer was precipitated twice in methanol and dried in vacuum at 25 °C for 1 day.

Preparation of Block Copolymers. The conditions of block copolymer synthesis (macro-RAFT agent, monomer, and concentrations) are given in Table 2. The same procedure as that used for the polymerization of the homopolymer was used except that ethyl acetate was used as a solvent. The polymer samples were purified by dialyzing against methanol for 3 days.

Hydrolysis of Polymers. The soluble PMOEP and PMAEP were hydrolyzed to poly(acrylic acid) (PAA) and poly(methacrylic acid) (PMA), respectively, by stirring in excess 5 M NaOH at 80 °C for 24 h. The resulting polymers were purified by dialyzing against water in a benzoylated dialysis tubing. Gel samples with high conversions were hydrolyzed with 10 M NaOH at 80 °C for 7 days.

Coupling of Block Copolymers to the Aminated Slide. 3-Aminopropyltrimethoxysilane (APS)-coated glass slides were kindly provided from Asper Biotech (ES). The reaction of PAAEMA and block copolymers with the aminated slide was done by immersing the slide in a polymer solution in dry dimethyl formamide (DMF) to react the primary amine on the glass surface with ketone on PAAEMA to form

Table 1. Experimental Conditions of MAEP and MOEP Polymerization Reactions and Characteristics of the Obtained Polymers[a−c]

							theoretical	experimental[e]		elemental analyses[f]			ICP[f]
expt	monomer	RAFT	[RAFT] (mol/L)	time (h)	conv (%)	characteristics	Mn[d]	Mn	PDI	%C	%H	%S	%P
1	MAEP			3	90	gel		125110[g]	2.98[g]	35.6 (30.6)	5.5 (4.6)	0	9.5 (15.8)
2	MAEP	1-PEPDA	1×10^{-2}	9	83	soluble	7325	5505	1.46	39.3 (31.3)	5.9 (4.6)	0.2 (0.3)	7.0 (15.6)
3	MAEP	1-PEPDA	2×10^{-2}	10	84	soluble	4113	5490	1.23				
4	MAEP	CDB	1×10^{-2}	40	35	soluble	3532	1331	1.22				
5	MOEP			3	96	gel		214783[g]	2.07[g]	37.7 (34.3)	5.9 (5.3)	0	11.2 (14.8)
6	MOEP	1-PEPDA	1×10^{-2}	0.7	23	gel	2499	262892	1.82				
				2	44	gel	4545	99938	3.63				
				7	81	gel	8502			37.6 (34.3)	5.9 (5.3)	0	11.5 (14.8)
7	MOEP	1-PEPDA	2×10^{-2}	7	95	gel							
8	MOEP	CDB	1×10^{-2}	20	74	soluble	7780	10655	1.94	38.3(33.4)	6.0 (5.0)	0.1 (0.3)	9.9 (13.9)
9	MOEP	CDB	2×10^{-2}	36	44	soluble	2438	2787	1.84				
	MAEP									29.3 (30.6)	4.9 (4.6)		15.9 (15.8)
	MOEP									34.5 (34.3)	5.5 (5.3)		14.7 (14.8)

[a] [MAEP] = 1.01 mol/L. [b] [MOEP] = 0.96 mol/L. [c] Solvent = methanol, [AIBN] = 2×10^{-3}, reaction temperature = 60 °C. [d] Theoretical M_n was calculated as conversion × a × [monomer]/[RAFT] + b; a = 94 or 108 (molecular weight of sodium acrylate for MAEP or sodium methacrylate for MOEP), and b = 106 or 174 (molecular weight of the polymer end groups after hydrolysis for 1-PEPDA or CDB). [e] Polymers were hydrolyzed for GPC analysis with 5 M NaOH at 80 °C for 24 h. [f] Values in parentheses are the calculated values. [g] After hydrolysis with 10 M NaOH.

Table 2. Experimental Conditions of Chain Extension Reactions and Molecular Weight of the Obtained Polymers after Hydrolysis

					[M]	[RAFT]	[AIBN]	time	conv	theoretical			units	
expt	macro-RAFT	Mn	PDI	monomer	(mol/L)	(mol/L)	(mol/L)	(min)	(%)	Mn	Mn[a]	PDI	PAAEMA	PMOEP/PMAEP
10	CDB			AAEMA	3.4	0.15	0.019	980	44	2200	5058[b]	1.13	22	
11	PAAEMA−X[c]	5058[b]	1.13	MAEP	0.53	0.005	0.001	270	40	6711	11857	1.38	22	99
12	PAAEMA−X[c]	5058[b]	1.13	MAEP	0.53	0.005	0.001	545	66	9302	17569	1.38	22	159
13	PMOEP−X[c]	10655[a]	1.94	AAEMA	0.22	0.005	0.0006	160	20	6664	22474	1.38	109	97
14	PAAEMA−X[c]	5058[b]	1.13	MOEP	0.49	0.005	0.001	180	39	6857	19329	1.41	22	155

[a] Mn after hydrolysis obtained by aqueous GPC. [b] Mn without hydrolysis obtained by GPC with THF as a solvent. [c] Note: X ≡ SC(Ph)=S.

an unstable imine. This linkage was then stabilized by mild reduction with addition of $NaCNBH_3$ to form stable secondary amine bonds. The slides were then washed thoroughly with DMF, rinsed with acetone, and dried. The reaction of PMOEP with the aminated slide was done by immersing the slide in a PMOEP solution in dry DMF. The slides were then washed thoroughly with DMF, rinsed with acetone, and dried.

Simulated Body Fluid (SBF) Experiments. The simulated body fluid was prepared according to the method described by Kim et al.[22] Chemicals were dissolved in MilliQ water (that had been boiled for 1 h prior to preparation) and buffered with HEPES (2-[4-(2-hydroxyethyl)-1-piperazinyl]ethanesulfonic acid) and 1 M NaOH at pH = 7.4 at 36.5 °C. The insoluble gels (expts 1 and 7) were used as prepared. The soluble polymers (expts 2 and 6) were cast from methanol solution onto glass substrate, and these samples were left on the substrates for the mineralization study. Approximately 10 mL of SBF solution was added to a 15 mL polystyrene tube containing a polymer sample. The tubes were immersed in a water bath at 36.5 ± 0.2 °C for a period of 7 days. The SBF solution was changed every 2 days. After 7 days, the polymers were washed by soaking in MilliQ water for 10 min, three times. The polymers were subsequently dried in a vacuum oven at 40 °C to constant weight.

Analytical Techniques. *FT-Raman Spectroscopy.* To obtain the degree of conversion, samples were prepared in ampules and FT-Raman spectra (PE Spectrum 2000 NIR FTIR, 64 scans, 8 cm^{-1} resolution, wavenumber range 4000−360 cm^{-1}) were recorded at various time points. Spectral information was extracted by means of spectral analysis software (GRAMS/32, Galactic Industries Corp., Salem, NH). The area under the vinyl peak at 1640 cm^{-1} that was normalized to the non-changing solvent signal at 1000 cm^{-1} was used for the conversion calculation. In addition, one sample for each reaction condition was polymerized in situ in an FT-Raman spectrometer (16 scans, 8 cm^{-1} resolution, wavenumber range 4000−360 cm^{-1}) at 60 °C to obtain a conversion/time curve. Spectra were collected every 3 min.

Gel Permeation Chromatography (GPC). Average molar mass and molar mass distributions of the hydrolyzed polymers were measured by GPC on a Waters system (Alliance GPCV 2000) equipped with three Ultrahydrogel columns (7.8 × 300 mm), a UV detector, and a refractive index (RI) detector. The sample was prepared by diluting the polymer solution with 5 mM NaOH to obtain a 10 mg/mL solution. The analyses were carried out in 5 mM NaOH solution at 60 °C, with a flow rate of 0.5 mL/min. Calibration was relative to 10 PAA standards (Mn range 830−888 900) (Polymer Standards Service, U.S.A.).

Elemental Analyses. Elemental carbon, hydrogen, and sulfur were determined using a Carlo Erba elemental analyzer model 1106. Elemental phosphorus was determined using an ICPAES Spectro spectroflame P instrument using a forward power of 1200 W, a flow rate of 1.0 mL/min, and a Meinhard concentric nebulizer. Soluble polymers, monomers, and standards were prepared in methanol. The insoluble gels were acid-digested prior to the characterization.

Scanning Electron Microscopy with Energy-Dispersive X-ray Analysis. SEM/EDX (FEI Quanta 200 Environmental SEM equipped with an Evarhart Thomley secondary-electron detector) was performed at 10 kV to examine the morphology of the calcium phosphate deposit and to obtain the elemental composition of the CaP minerals on the surface.

Fourier Transform Infrared Spectroscopy-Attenuated Total Reflectance. A Nicolet Fourier transform infrared spectrometer equipped with a diamond ATR (refractive index of 2.41 at 1000 nm and an average angle of incidence of 50°) was used to analyze the mineral deposits (64 scans, 4 cm^{-1} resolution, wavenumber range 4000−525 cm^{-1}). The depth of penetration was calculated to be between 2.85 (525 cm^{-1}) to 0.37 μm (4000 cm^{-1}), for an estimated refractive index of the polymer/CaP phase of 1.5.

X-ray Photoelectron Spectroscopy. XPS spectra of the aminated slides with and without polymers were recorded by Kratos Axis Ultra X-ray photoelectron spectrometer (XPS) with a monochromated Al Kα X-ray source (1486.6 eV) at 15 kV and 15 mA (150 W). The survey scans were collected at 1200−0 eV with 1.0 eV steps at a pass energy of 160 eV and the narrow scans at 0.1 eV steps at a pass energy of 20 eV. Vision 2 software was used for data acquisition and processing.

The binding energies were charge-corrected using a C1s peak (285 eV). N1s high-resolution spectra were resolved into individual Gaussian−Lorentzian peaks using a least-squares fitting program (PeakFIT, Jandell Scientific Software). Component energies, number of peaks, and peak widths (1.5) were fixed as obtained from Vision 2 software, and only peak heights were optimized. Peak fit results were imported into a graphic software package for final illustrations.

Time-of-Flight Secondary-Ion Mass Spectrometry (ToF-SIMS). The ToF-SIMS analyses were performed with a PHI TRIFT II (model 2100) spectrometer (PHI Electronics Ltd., U.S.A.) equipped with ^{69}Ga liquid metal ion gun (LMIG). A 15 keV pulsed primary ion beam was used to desorb and ionize species from a sample surface. Pulsed, low-energy electrons were used for charge compensation. Stainless steel grids were additionally used to minimize charging effects. Mass axis calibration was done with CH_3^+, $C_2H_5^+$, and $C_3H_7^+$ in positive mode and with CH^-, C_2H^-, and Cl^- in negative mode of operation. A mass resolution $m/\Delta m$ of ~4500 at nominal $m/z = 27$ amu ($C_2H_3^+$) was typically achieved.

Results and Discussion

RAFT-Mediated Polymerization of MAEP and MOEP. The MAEP homopolymerizations were carried out in the presence of either 1-PEPDA or CDB with AIBN as initiator in methanol at 60 °C. The experimental conditions and characteristics of the polymer structure (i.e., either cross-linked or soluble in the solvent) are given in Table 1. A control MAEP polymerization was carried out under the same experimental conditions as above but in the absence of any RAFT agent. This experiment resulted in a rapid polymerization, reaching 100% conversion in under 1 h (see curve a, Figure 1A) and the formation of an insoluble cross-linked gel. Polymerization of MAEP in the presence of 1-PEPDA at two different concentrations gave polymers that were soluble in methanol with no gel formation. There is a marked increase in the inhibition times with increased 1-PEPDA (Figure 1A, curves b and c) from approximately 50 min (at [1-PEPDA]= 1×10^{-2} M) to 120 min (at [1-PEPDA]= 2×10^{-2} M), suggesting that the leaving radical R ($Ph(CH_3)CH^{\bullet}$) is slow to reinitiate polymerization.[25−27] Although PMAEP was soluble in water, the eluent used in the GPC analysis, it was hydrolyzed with 5 M NaOH to give poly(acrylic acid) (PAA), and its molecular weight distribution was determined absolutely using a PAA calibration curve (Table 1). (This method was used in the analysis of all the PMAEP and PMOEP samples, and the disappearance of the of methylene resonances ($\delta = 3.6-4.6$) from the side chain in the ^1H NMR spectra (data shown in the Supporting Information) showed that the polymer is converted to the acid form). The M_n increased linearly with conversion for the two 1-PEPDA concentrations, and the PDIs decreased from 1.3 to approximately 1.2 over the conversion range. Although the M_n profile for the 1-PEPDA at 1×10^{-2} M was close to theory (solid line, Figure 1B), at the higher concentration of 1-PEPDA the experimental M_n's were greater than theory by a factor of approximately 2 (dotted line, Figure 1B) and converged toward the theoretical line above conversions of 70% due to the increased amount of dead polymer arising from initiator-derived radicals. Polymerization of MAEP with CDB gave a much slower rate of polymerization to that of 1-PEPDA but with no inhibition period; the M_n was low (1331, expt 4 in Table 1), and the PDI was close to 1.22. This suggests that either slow fragmentation[28] or intermediate radical termination[29] plays a role in CDB-mediated polymerization, which is further complicated by impurities found in the preparation and storage of CDB.[30] There is still debate concerning the actual mechanism of inhibition and retardation, which has been thoroughly reviewed.[31]

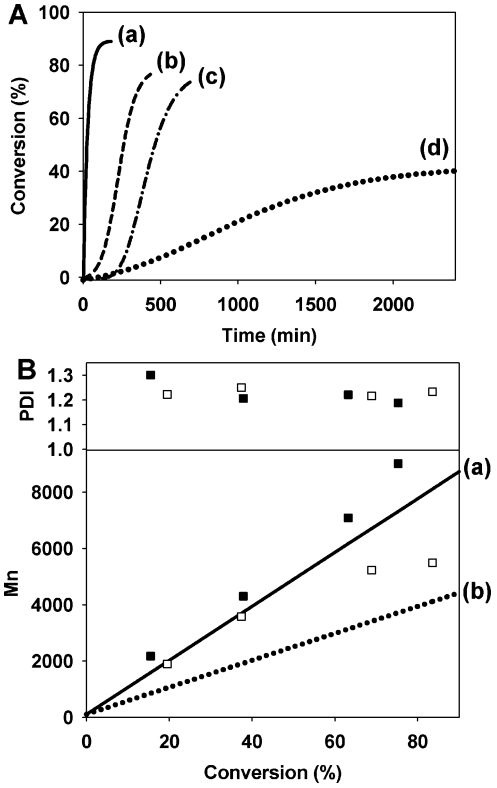

Figure 1. (A) Conversion vs time of MAEP polymerization in methanol using the RAFT agent 1-PEPDA or CDB and AIBN as initiator: (a) no RAFT (expt 1), (b) [1-PEPDA] = 1×10^{-2} M (expt 2), (c) [1-PEPDA] = 2×10^{-2} M (expt 3), and (d) [CDB] = 1×10^{-2} M (expt 4). (B) M_n and PDI of PMAEP polymerized with 1-PEPDA after hydrolysis: (a) [1-PEPDA] = 1×10^{-2} M (expt 2 ■) and (b) 2×10^{-2} M (expt 3 □). The lines show the theoretical evolution of M_n with conversion for PAA. The theoretical M_n was calculated as conversion × 94 × [MAEP]/[1-PEPDA] + 106; 94 is the molecular weight of sodium acrylate, and 106 is the molecular weight of the polymer end groups after hydrolysis.

The MOEP homopolymerization was carried out in the presence of either 1-PEPDA or CDB with AIBN as initiator in methanol at 60 °C. The experimental conditions and characteristics of the polymer structure are given in Table 1. In the absence of RAFT agent, the polymerization was fast and reached high conversion (over 85%) after 200 min (curve a, Figure 2A) resulting in the formation of an insoluble gel. Polymerization in the presence of 1-PEPDA showed only a slight decrease in rate with increased RAFT agent concentration (Figure 2A, curves b and c), suggesting that reinitiation is not the rate-determining step. The polymers formed for the two 1-PEPDA concentrations were cross-linked gels. When CDB is used as the RAFT agent at the same concentrations, the polymer was found to be soluble but the rates of polymerization were severely retarded (Figure 2A, curves d and e) due to either slow fragmentation or intermediate radical termination. The M_n values increased linearly with conversion and were close to theory for both CDB concentrations (Figure 2B), suggesting that the RAFT agent had been consumed early in the polymerization. This is in contrast to what is usually found for methacrylate monomers,[25] where the slow fragmentation of the R group on the RAFT agent gives an M_n profile similar to that for conventional chain transfer agents. However, for MOEP, the PDI profiles deviate from ideal "living" behavior. The PDI profiles (Figure 2B) are similar for the two CDB concentrations and increase from 1.6 at low conversion to over 2 at high conversion. The reason for this is unclear.

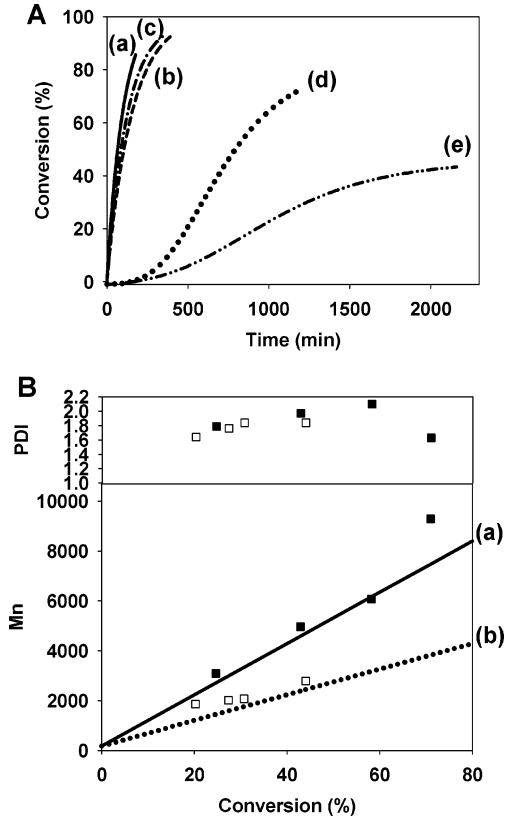

Figure 2. (A) Conversion vs time of MOEP polymerization in methanol using the RAFT agent 1-PEPDA or CDB and AIBN as initiator: (a) no RAFT (expt 5), (b) [1-PEPDA] = 1×10^{-2} M (expt 6), (c) [1-PEPDA] = 2×10^{-2} M (expt 7), (d) [CDB] = 1×10^{-2} M (expt 8), and (e) [CDB] = 2×10^{-2} M (expt 9). (B) M_n and PDI of PMOEP polymerized with CDB after hydrolysis: (a) [CDB] = 1×10^{-2} M (expt 8 ■) and (b) 2×10^{-2} M (expt 9 □). The solid lines show the theoretical evolution of M_n with conversion calculated as conversion × 108 × [MOEP]/[CDB] + 174; 108 is the molecular weight of sodium methacrylate, and 174 is the molecular weight of polymer end groups after hydrolysis.

Mechanism of Gel Formation. It has been proposed that phosphate-containing monomers and other monomers (e.g., HEMA[32]) cross-link in free radical polymerizations due to the presence of either small amounts of residual diacrylate or dimethacrylate contaminants or as a result of chain transfer to monomer or polymer.[7,8] To gain some insight into the mechanism of gel formation, the gel polymers were hydrolyzed with either 5 or 10 M NaOH for 7 days at 80 °C. This quite harsh treatment of the polymer should result in the conversion of all ester groups in the polymer side chains to carboxylic acid groups. Therefore, if as a result of this treatment the polymers become soluble in good solvents, we can confidently infer that the cross-links are formed through the polymer side chains and not the backbone carbons.

Hydrolysis of PMAEP (expt 1, Table 1) gives an M_n close to 1.25×10^5 and a PDI of 2.98, with a similar result for PMOEP (expt 5). Hydrolysis of PMOEP made using 1-PEPDA after 23% conversion gave an M_n of 2.6×10^5 (PDI of 1.82) that decreased to 9.99×10^4 (PDI of 3.36) after 44% conversion. These results suggest that most if not all cross-linking of MOEP and MAEP in both the presence and absence of RAFT agent is through the side chain and not through the polymer backbone. It can also be seen that the MOEP polymerization using 1-PEPDA gave M_n's close to that of the free radical polymerization, suggesting that these polymerizations are not controlled and 1-PEPDA is an ineffective RAFT agent for this monomer.

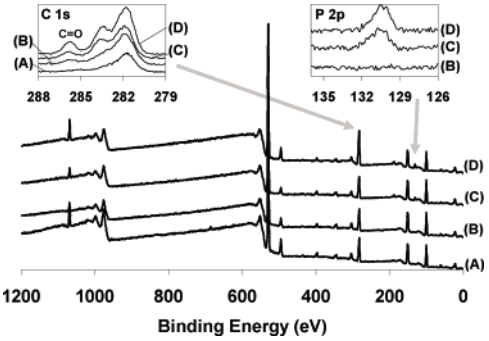

Figure 3. XPS spectra of aminated slides (A) as received, (B) PAAEMA (expt 10) attached, (C) PMOEP (expt 8) attached, and (D) PMOEP-*b*-PAAEMA (expt 13) attached.

On the basis of these data and the M_n data in Table 1, it seems that cross-linked polymer forms when high molecular weight polymer is formed and soluble polymer when molecular weights below 20 K are produced. Therefore, we can exclude chain transfer reactions to polymer (or even monomer) as this would be conversion (or more precisely dependent upon the weight fraction of polymer in the reaction mixture) and not molecular weight dependent. The most likely mechanism for cross-linking results from the presence of residual dimethacrylate and diacrylate monomers formed during the synthesis of MOEP and MAEP, respectively. Cross-linking in this case is inversely dependent upon the chain length of the polymer: the greater the chain length the greater the conditional probability for cross-linking.[33,34] Quantification of the degree of cross-linking in our systems is difficult due to the unknown amounts of diene present as well as the reactivity of their double bonds.

Synthesis of Block Copolymer of MAEP and MOEP with AAEMA. AAEMA has a ketone side group that can react under mild conditions with amines to give an imine, which can then be reduced to more stable secondary amines — a reaction that has previously proven successful for soluble amine reactants.[35] Therefore, we prepared a selection of block copolymers, P(MOEP-*b*-AAEMA) and P(AAEMA-*b*-MAEP), to immobilize the linear PMOEP and PMAEP on aminated surfaces suitable for SBF studies. The homopolymerization of AAEMA with CDB (expt 10, Table 2) gave an M_n close to theory with a low PDI (1.13). This polymer was further chain extended with MAEP (expts 11 and 12) and MOEP (expt 14). The M_n's for these polymerizations were double that of theory, and the PDIs were close to 1.38, which are satisfactory for our purpose since the majority of chains contain both MOEP and AAEMA units. It was also necessary to couple a P(AAEMA) block of much greater than 22 units. Therefore, PMOEP made with CDB (expt 13) was chain extended with AAEMA to give an M_n of 22 474 (109 units of AAEMA) and PDI of 1.38, again an acceptable PDI for our purpose.

Coupling of Block Copolymers to the Aminated Slides. Coupling of the block copolymers to the aminated slides was carried out in dry DMF at room temperature followed by mild reduction with $NaCNBH_3$ to convert the unstable imines to more stable secondary amines. The successful immobilization of the block copolymers onto the aminated slides was verified from the XPS spectral changes. The XPS spectrum of an unreacted aminated slide showed the presence of N and C from the APS, as well as O, Si, and small amounts of Na and Ca from the glass slide. After reaction with the block copolymers, the increase in the C atom %, as well as the appearance of P was concomitant with a decrease in the O, N, and Si (Figure 3 and Table 3). PAAEMA and PMOEP homopolymers were also

Table 3. XPS Data: Atomic Percent of Element Concentrations from XPS Survey Scans

polymer attached	Na	O	N	Ca	C	P	Si
none	3.9 8	54.38	2.5 7	0.8 8	22.33		15.86
PAAEMA (expt 10)	1.6 4	49.71	1.7 8	1.1 9	26.31		19.38
PMOEP (expt 8)	1.8 4	49.94	1.6 7	1.0 2	26.14	1.3 0	18.10
PAAEMA−PMAEP (expt 11)	2.2 5	47.54	1.5 4	0.7 6	30.73	0.9 8	16.21
PAAEMA−PMAEP (expt 12)	1.9 0	46.46	1.4 8	0.8 1	32.31	0.8 9	16.14
PMOEP−PAAEMA (expt 13)	3.5 2	44.29	1.4 9	0.5 4	35.95	1.4 5	12.79
PAAEMA−PMOEP (expt14)	3.2 5	38.64	1.5 0	0.3 1	46.05	1.7 9	8.47

Table 4. XPS Data: Normalized Atomic Percent of Various Nitrogen Species Determined through Curve Fitting to the N1s Peak

polymer attached	N1[a]	N2[b]	N3[c]
none	46.3	27.3	26.4
PAAEMA (expt 10)	55.2	22.7	22.1
PMOEP (expt 8)	30.6	26.9	42.5
PAAEMA−PMAEP (expt 11)	40.5	26.3	33.2
PAAEMA−PMAEP (expt 12)	37.2	21.9	40.9
PMOEP−PAAEMA (expt 13)	41.7	26.7	31.7
PAAEMA−PMOEP (expt 14)	38.3	26.8	34.9

[a] 399.5−399.7 eV. [b] 400.9−401.0 eV. [c] 401.9−402.6 eV.

reacted with the slides as controls. The high-resolution spectra of the N1s peak of all the samples (Figure 4) required three peaks for the fit, and these peaks were assigned to amine (399.6 eV), amide (401 eV), and the protonated amine (402 eV).[36]The shape of the N1s peak changes depending on which polymer is attached to the slide. The relative ratios of the fitted nitrogen peaks are given in Table 4. In comparison to the aminated slide, the attachment of PAAEMA to the slide caused a slight decrease in both amide and protonated amine peaks in agreement with coupling of this homopolymer through reductive amination. The attachment of PMOEP caused an increase in the protonated amine peak. It is likely that ionic interactions between deprotonated phosphate groups and protonated amine groups are in fact occurring. In the dry aprotic solvent dimethyl formamide (DMF), proton transfer from the phosphate groups to the amine groups can mediate the reaction. In the case of block copolymers, an increase in the peak assigned to the protonated amine compared to that of the aminated slide was also observed. However, this increase was not as large as for the PMOEP-attached slide, thus indicating that both reductive amination and ionic interactions took place. In these systems it appears that the PMOEP or PMAEP portions of the block copolymers are prevented from extending out from the surface of the glass slide due to the ionic interactions.

Both the aminated and PMOEP−PAAEMA block copolymer-functionalized glass slides (expt 13) were subjected to ToF-SIMS analysis. The negative mass spectrum of the block copolymer-functionalized slide revealed two new intense peaks corresponding to phosphorus moieties, namely, at 63 *m*/*z* (PO_2^-) and at 79 *m*/*z* (PO_3^-), compared to the spectrum of the unfunctionalized aminated slide. The mass peak at 79 *m*/*z* was imaged over an area of 100 μm × 100 μm and showed (Figure 5) that the lateral distribution of phosphate groups was uniform across the surface of the slide.

SBF Studies of Phosphate Polymers. Mineralization is a complicated process which, although extensively studied over the years, is still not completely understood. The need to predict how a material will behave in vivo has led to the use of the

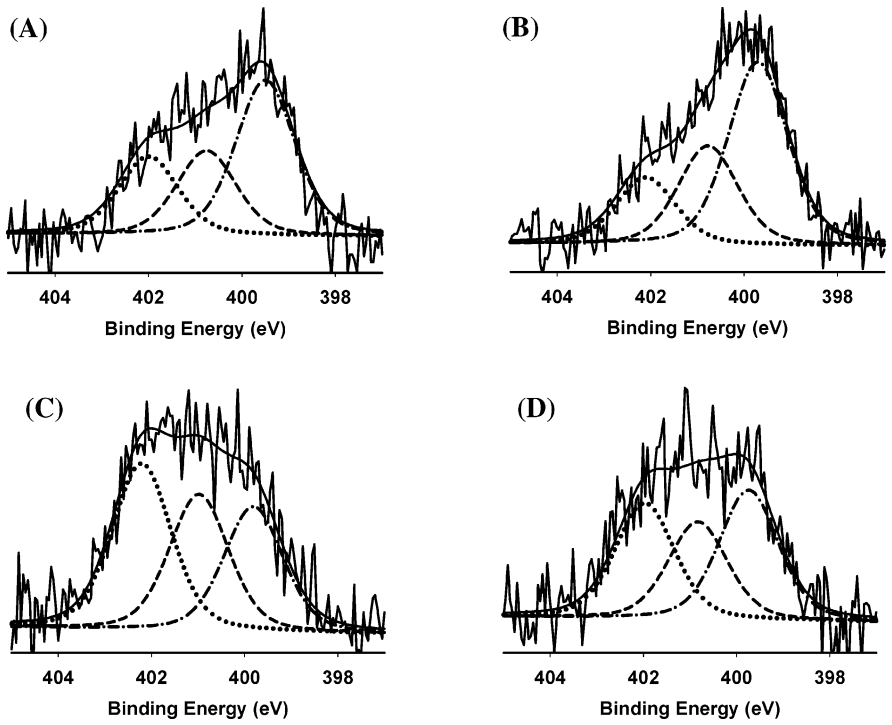

Figure 4. N 1s narrow scans of aminated slides (A) as received, (B) PAAEMA (expt 10) attached, (C) PMOEP (expt 8) attached, and (D) PMOEP-*b*-PAAEMA (expt 13) attached.

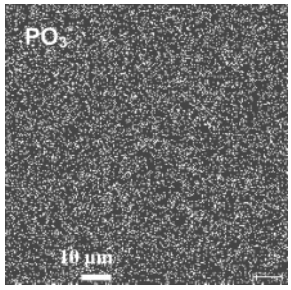

Figure 5. Lateral distribution of the phosphate groups (PO_3^-) across the sample PMOEP−PAAEMA (expt 13) attached to an aminated slide (analyzed area 100 μm × 100 μm).

so-called simulated body fluid (SBF) techniques as the most common method for testing calcium phosphate mineralization in vitro.[22] The formation of calcium−phosphate (CaP) minerals or a bonelike apatitic layer in SBF is accepted as an indication of the bone-bonding ability of the material in vivo.[37] The effect of negatively charged functional groups such as carboxylate and phosphate on the calcification of polymeric materials has recently been the subject of an excellent review by Chirila and Zainuddin.[12] Although the incorporation of phosphorus-containing moieties has been shown to lead, in vitro, to the enhanced calcification of naturally occurring materials such as cotton,[38,39] bamboo,[40,41] and chitin,[42] the calcification results for synthetic polymers is less well-studied and somewhat controversial.[43] As Chirila pointed out in his review "the effect of the phosphate group may be more complicated than initially thought".

Before undertaking SBF studies it is important to characterize the polymer thoroughly since factors such as the amount and distribution of phosphate groups will affect mineralization. Since the C, H, and P % of monomers agreed with the theoretical values, it is clear from the elemental analysis of the polymers that some loss of phosphorus has occurred in all systems (Table 1). This phenomenon was most pronounced for the soluble polymers produced by RAFT-mediated synthesis due to the fact that the phosphate groups are more accessible to reaction compared to those in the gels. In addition, as a result of the

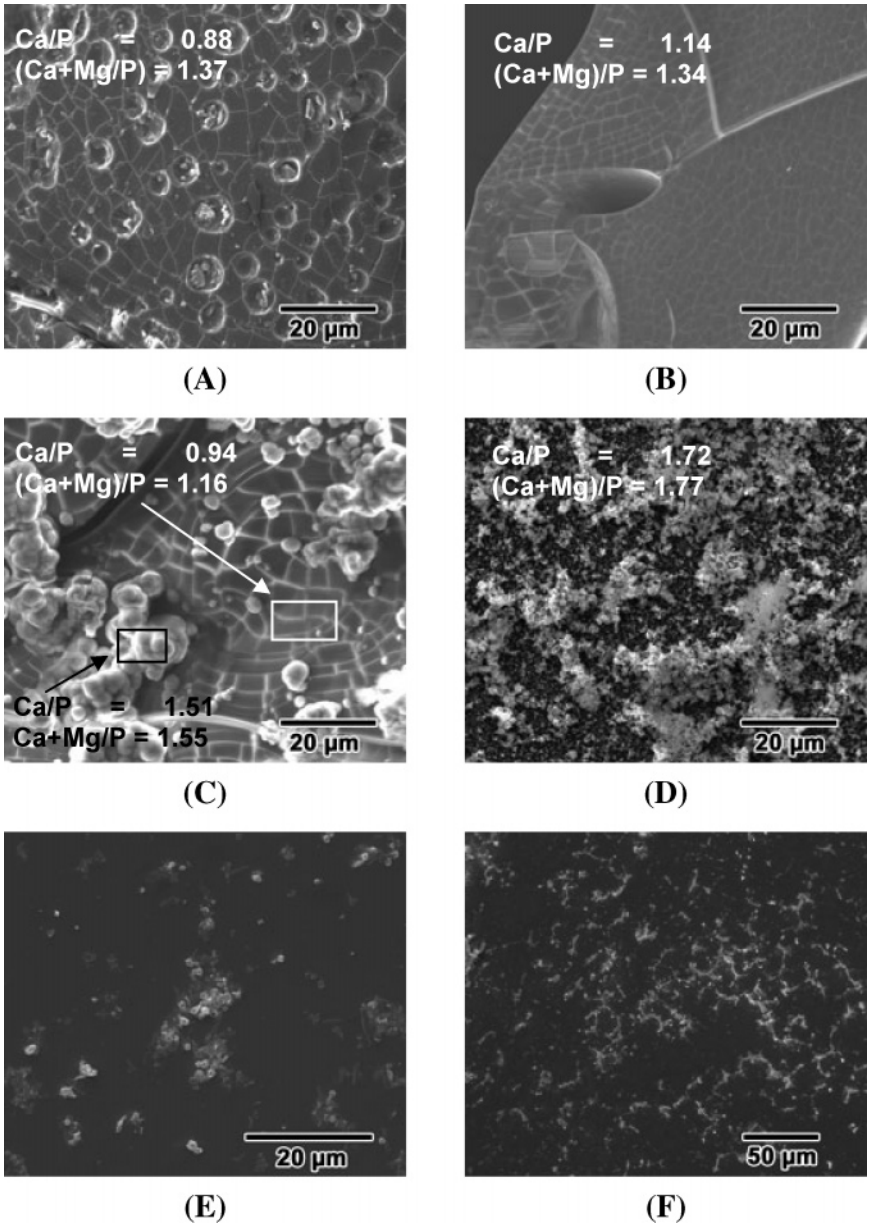

Figure 6. SEM images of minerals formed on the polymer surfaces after 7 days immersion in SBF: (A) PMAEP gel (expt 1), (B) PMAEP film (expt 2) (this was done in 1.5× SBF), (C) PMOEP gel (expt 7), and (D) PMOEP film on a glass surface (expt 8). SEM images of aminated slides after 2 weeks in SBF (E) PMOEP−PAAEMA (expt 13) attached and (F) as received.

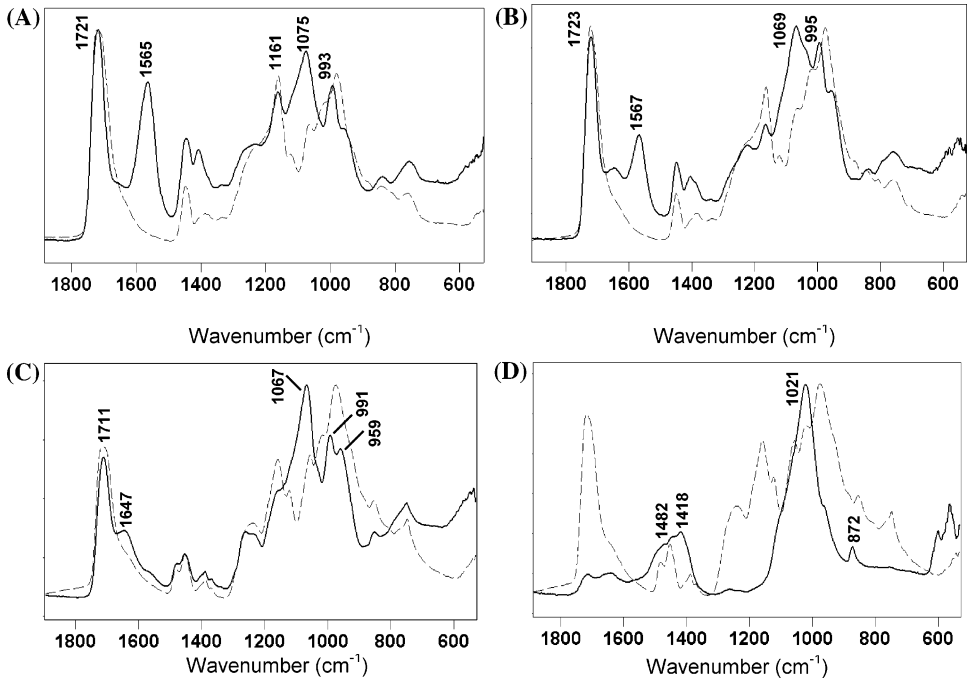

Figure 7. ATR-FTIR spectra of polymer samples after 7 days immersion in SBF (solid line) and initial polymers (dotted line): (A) PMAEP gel (expt 1), (B) PMAEP film (expt 2) (this was done in 1.5× SBF), (C) PMOEP gel (expt 7), and (D) PMOEP film on a glass surface (expt 8).

long RAFT polymerization times, loss of the phosphate groups could be attributed to hydrolysis by their acidic protons in the presence of trace amounts of water. It was also noted that the acrylate systems were more prone to such hydrolysis than the corresponding methacrylates. This is in agreement with the general observation that methacrylate polymers are much more stable than acrylate polymers toward spontaneous hydrolysis in aqueous media.[21] From the FTIR investigation, it was evident that both linear and gel PMAEP contained a high proportion of carboxylic acid groups and thus must have undergone hydrolysis at the ester bond (described below, Figure 7, parts A and B).

Mineralization of a series of phosphate-containing linear and cross-linked polymers was investigated using SBF in order to evaluate the effect of cross-linking. The linear polymer samples for SBF were prepared as either cast films or block copolymers attached to aminated glass slides. Linear PMAEP film was soluble in SBF, hence a modified SBF solution 1.5 times the concentration of normal SBF was used. EDX elemental analysis revealed the presence of C, O, P, Ca, and small amounts of Mg and Na in all homopolymer samples after SBF immersion. The presence of carbon is due mainly to the sample coating used for SEM/EDX analysis but may also be from the polymer and/or carbonate ions. In mineralization studies, Mg^{2+} substitution for Ca^{2+} within a CaP lattice is often observed,[44] and it is therefore necessary to evaluate both the Ca/P and (Ca + Mg)/P ratios.

Thin layers of CaP mineral were observed on the surfaces of the PMAEP gel (expt 1) and the soluble PMAEP (expt 2) film (Figure 6, parts A and B). The tilelike morphology has been observed previously on PMAEP-*g*-ePTFE.[15] These mineral layers had Ca/P and (Ca + Mg)/P ratios of 0.88−1.14 and 1.34−1.37, respectively (insets in Figure 6), indicating that this mineral phase is possibly either brushite ($CaHPO_4 \cdot H_2O$) or monetite ($CaHPO_4$). This is confirmed by the ATR-FTIR spectra which show a band around 991−995 cm^{-1}, together with shoulders at higher wavenumber on the 1070 cm^{-1} band (Figure 7, parts A and B).[45] Brushite, which is a thermodynamically unstable phase, has been proposed as a precursor of the more stable HAP in an in vitro mineralization mechanism.[46] Another important feature of the FTIR spectra of the SBF-treated PMAEP samples (Figure 7, parts A and B) is the new band at 1565−1567 cm^{-1} corresponding to the carbonyl vibration of a carboxylate group. This indicates that large amounts of the PMAEP side chains were hydrolyzed at the ester bond. Deprotonation of these carboxylic acid groups occurs as a consequence of Ca^{2+} binding similar to that observed previously for PAA-*g*-ePTFE.[15]

The PMOEP gel was covered with a tilelike mineral layer (Ca/P = 0.94 and (Ca + Mg)/P = 1.16) similar to those observed on the PMAEP samples. In addition, secondary growth of round mineral nodules of various sizes (ø ∼ 2−5 μm), including some large clusters, was observed (Figure 7C). The spherical morphology is often observed for HAP formed in vitro,[47,48] and this observation as well as the Ca/P and (Ca + Mg)/P ratios (1.51 and 1.55, respectively) suggests that the minerals are nonstoichiometric HAP. Similar secondary growth has been observed on PMAEP-*g*-ePTFE.[15]

ATR-FTIR spectra of the PMAEP and PMOEP gels and linear PMAEP film all show a new band around 1070 cm^{-1} after SBF treatment (Figure 7A−C). According to the literature this band does not correspond to phosphates in any of the previously identified CaP phases.[45] The band cannot be ascribed to the phosphate groups of the polymers interacting with calcium ions since experiments have shown that such an interaction results in the large broad acidic phosphate vibration around 975 cm^{-1} giving rise to two strong bands at 1060 and 962 cm^{-1}, corresponding to the out-of-phase stretching and the in-phase stretching vibrations,[49] respectively (data not shown). In the soluble PMAEP sample (Figure 7B), the band at 1069 cm^{-1} has a shoulder at 1036 cm^{-1}. However, it is not possible to identify a mineral phase based one band. The bands around 1650 cm^{-1} observed in all samples were assigned to water bound to either the CaP mineral or the polymers in their deprotonated state.[18]

After 7 days the SBF-treated soluble PMOEP (expt 8) cast on the glass surface was also covered with a large amount of spherical mineral clusters. Its morphology was much smaller in diameter than that formed on the PMOEP gel, and it had Ca/P and (Ca + Mg)/P ratios of 1.72 and 1.77, respectively,

similar to the theoretical value for HAP (i.e., 1.67). The FTIR spectrum of this sample shows a dramatic decrease of polymer bands indicating large amount of mineral formation on this sample (Figure 7D). There was a broad band at 1020 cm^{-1} which can be assigned to the P−O stretching of phosphates in HAP, and bands at 1482, 1418, and 872 cm^{-1} corresponding to carbonate vibrations of carbonated HAP. This is analogous to an earlier result for MOEP grafted onto ePTFE in methanol.[14] Interestingly, that study also showed that PMOEP-*g*-ePTFE formed in other solvents did not induce HAP nucleation, but rather different CaP phases, suggesting that the graft copolymer formed in methanol is structurally more similar to the linear PMOEP of this study.

The different mineralization outcomes of the four samples described above are most likely due to a combination of factors including phosphate content and distribution as well as the degree of cross-linking. The PMOEP polymers had significantly less phosphorus loss (less than 30% of the theoretical value) than the PMAEP polymers (40% for the cross-linked system and 60% for the linear polymer). However, a high phosphate content did not necessarily result in large amounts of HAP nucleation. This was only observed for the linear PMOEP sample, thus leading to the conclusion that the degree of cross-linking also influences mineralization.

Block copolymers consisting of PMAEP or PMOEP and PAAEMA fixed on aminated slides showed sparse, patchy CaP mineral formation after up to 2 weeks in SBF. The scanning electron micrograph of the PMOEP−PAAEMA (expt 11, Table 2)-functionalized aminated slide after immersion in SBF is shown in Figure 6E; all other block copolymer samples showed similar results. It was not possible to evaluate the Ca/P ratio of the sparse mineral formed on the modified slides because the slides themselves contain high amounts of calcium. Although the control PAAEMA sample did not induce any CaP mineral formation, CaP was observed on the aminated slide after 2 weeks (Figure 6F). Interestingly, this mineral phase showed a distinctive morphology not seen in any of the phosphate-containing samples. Although amine groups are not as efficient at inducing CaP growth as phosphate and carboxylate groups, CaP nucleation has previously been observed on amine-terminated self-assembled monolayers.[50] We have been able to discount one possible explanation for the sparse mineralization of the block copolymers on the aminated slides, namely, possible inhomogeneously dispersed phosphate groups. ToF-SIMS of the PAAEMA−PMOEP aminated slide showed the distribution of phosphate groups to be uniform. It is more likely that ionic interactions between the phosphate block and the protonated amine groups leading to ion pairs prevents chelation of the calcium ions from the SBF solution. This finding supports Tanahashi and Matsuda's conclusion that the chelation of calcium ions by negatively charged groups plays an important role in biomaterial calcification.[50]

Conclusion

This is the first report of a RAFT-mediated polymerization of MAEP and MOEP monomers to give non-cross-linked (linear) polymers. In those cases where cross-linking did occur it was postulated that this occurred through residual diene monomers formed from the synthesis of MAEP and MOEP. To eliminate cross-linking in the presence of diene cross-linkers, the molecular weight must be kept low, which in our case is below 20 K. Above this molecular weight, cross-linked gels are observed. The mineralization behavior between cross-linked and linear PMAEP and PMOEP were compared.

In our ongoing studies on phosphate-containing polymeric materials it has become clear that the in vitro mineralization is influenced by factors other than the nature of the monomer. We have demonstrated that the amount of phosphate groups and the degree of cross-linking, as well as accessibility of the phosphates themselves, play an important role in both the amount and type of mineral formed. Not only do our in vitro mineralization results from this study correlate well with our previous work on grafted ePTFE membranes, they also indirectly clarify the structure of the grafted copolymers. In the case of the block copolymer attached to the aminated slides, we have highlighted the importance of accessible, ionic phosphate groups for calcium ion chelation and subsequent CaP nucleation.

Acknowledgment. The authors thank Mr. Marek Jasieniak and Professor Hans Griesser, Ian Wark Research Institute, University of South Australia, for their technical support with the ToF-SIMS analysis and for providing the ToF-SIMS image. Asper Biotech (ES) is acknowledged for providing aminated slides.

Supporting Information Available. ^1H NMR (400) MHz spectrum of linear PMAEP in methanol-d_4 and hydrolyzed PMAEP in D_2O (Figure S1). This material is available free of charge via the Internet at http://pubs.acs.org.

References and Notes

(1) Rixens, B.; Severac, R.; Boutevin, B.; Lacroix-Desmazes, P. *J. Polym. Sci., Part A: Polym. Chem.* **2006**, *44*, 13−24.
(2) Grøndahl, L.; Cardona, F.; Chiem, K.; Wentrup-Byrne, E. *J. Appl. Polym. Sci.* **2002**, *86*, 2550−2556.
(3) Nuttelman, C. R.; Benoit, D. S. W.; Tripodi, M. C.; Anseth, K. S. *Biomaterials* **2006**, *27*, 1377−1386.
(4) Stancu, I. C.; Filmon, R.; Cincu, C.; Marculescu, B.; Zaharia, C.; Tourmen, Y.; Basle, M. F.; Chappard, D. *Biomaterials* **2004**, *25*, 205−213.
(5) Wentrup-Byrne, E.; Grøndahl, L.; Suzuki, S. *Polym. Int.* **2005**, *54*, 1581−1588.
(6) Tretinnikov, O. N.; Kato, K.; Ikada, Y. *J. Biomed. Mater. Res.* **1994**, *28*, 1365−1373.
(7) Reghunadhan Nair, C. P.; Clouet, G.; Brossas, J. *J. Polym. Sci., Part A: Polym. Chem.* **1988**, *26*, 1791−1807.
(8) Pike, R. M.; Cohen, R. A. *J. Polym. Sci.* **1960**, *44*, 531−538.
(9) Nakamae, K.; Miyata, T.; Hoffman, A. S. *Macromol. Chem. Phys.* **1992**, *193*, 983−990.
(10) George, K. A.; Wentrup-Byrne, E.; Hill, D. J. T.; Whittaker, A. K. *Biomacromolecules* **2004**, *5*, 1194−1199.
(11) Nakamae, K.; Nizuka, T.; Miyata, T.; Furukawa, M.; Nishino, T.; Kato, K.; Inoue, T.; Hoffman, A. S.; Kanzaki, Y. *J. Biomater. Sci., Polym. Ed.* **1997**, *9*, 43−53.
(12) Chirila, T. V.; Zainuddin *React. Funct. Polym.*, in press.
(13) Kamei, S.; Tomita, N.; Tamai, S.; Kato, K.; Ikada, Y. *J. Biomed. Mater. Res.* **1997**, *37*, 384−393.
(14) Suzuki, S.; Grøndahl, L.; Leavesley, D.; Wentrup-Byrne, E. *Biomaterials* **2005**, *26*, 5303−5312.
(15) Grøndahl, L.; Cardona, F.; Chiem, K.; Wentrup-Byrne, E.; Bostrom, T. *J. Mater. Sci.: Mater. Med.* **2003**, *14*, 503−510.
(16) Matyjaszewski, K., Ed. *Controlled/Living Radical Polymerization: Progress in ATRP, NMP, and RAFT*; American Chemical Society: Washington, DC, 2000.
(17) Huang, J.; Matyjaszewski, K. *Macromolecules* **2005**, *38*, 3577−3583.
(18) Zhou, F.; Huck, W. T. S. *Chem. Commun.* **2005**, 5999−6001.
(19) Ma, I. Y.; Lobb, E. J.; Billingham, N. C.; Armes, S. P.; Lewis, A. L.; Lloyd, A. W.; Salvage, J. *Macromolecules* **2002**, *35*, 9306−9314.
(20) Stenzel, M. H.; Barner-Kowollik, C.; Davis, T. P.; Dalton, H. M. *Macromol. Biosci.* **2004**, *4*, 445−453.
(21) Yusa, S.; Fukuda, K.; Yamamoto, T.; Ishihara, K.; Morishima, Y. *Biomacromolecules* **2005**, *6*, 663−670.
(22) Kim, H. M.; Miyazaki, T.; Kokubo, T.; Nakata, T. *Bioceramics* **2000**, *13*, 47−50.
(23) Quinn, J. F.; Rizzardo, E.; Davis, T. P. *Chem. Commun.* **2001**, 1044−1045.
(24) Oae, S. Y. T.; Okabe, T. *Tetrahedron* **1972**, *28*, 3203.

(25) Moad, G.; Chiefari, J.; Chong, Y. K.; Krstina, J.; Mayadunne, R. T. A.; Postma, A.; Rizzardo, E.; Thang, S. H. *Polym. Int.* **2000**, *49*, 993−1001.
(26) Theis, A.; Feldermann, A.; Charton, N.; Stenzel, M. H.; Davis, T. P.; Barner-Kowollik, C. *Macromolecules* **2005**, *38*, 2595−2605.
(27) Monteiro, M. J. *J. Polym. Sci., Part A: Polym. Chem*. **2005**, *43*, 3189−3204.
(28) Barner-Kowollik, C.; Quinn, J. F.; Morsley, D. R.; Davis, T. P. *J. Polym. Sci., Part A: Polym. Chem.* **2001**, *39*, 1353−1365.
(29) Monteiro, M. J.; de Brouwer, H. *Macromolecules* **2001**, *34*, 349−352.
(30) Plummer, R.; Goh, Y.-K.; Whittaker, A. K.; Monteiro, M. J. *Macromolecules* **2005**, *38*, 5352−5355.
(31) Barner-Kowollik, C.; Buback, M.; Charleux, B.; Coote, M. L.; Drache, M.; Fukuda, T.; Goto, A.; Klumperman, B.; Lowe, A. B.; McLeary, J. B.; Moad, G.; Monteiro, M. J.; Sanderson, R. D.; Tonge, M. P.; Vana, P. *J. Polym. Sci., Part A: Polym. Chem.* **2006**, *44*, 5809−5831.
(32) Robinson, K. L.; Khan, M. A.; de Paz Banez, M. V.; Wang, X. S.; Armes, S. P. *Macromolecules* **2001**, *34*, 3155−3158.
(33) Landin, D. T.; Macosko, C. W. *Macromolecules* **1988**, *21*, 846−851.
(34) Li, W.-H.; Hamielec, A. E.; Crowe, C. M. *Polymer* **1989**, *30*, 1518−1523.
(35) Park, J. P.; Monteiro, M. J.; van Es, S.; German, A. L. *Eur. Polym. J.* **2001**, *37*, 965−973.
(36) Keen, I.; Broota, P.; Rintoul, L.; Fredericks, P.; Trau, M.; Grøndahl, L. *Biomacromolecules* **2006**, *7*, 427−434.
(37) Hench, L. L. *J. Am. Ceram. Soc.* **1998**, *81*, 1705−1728.
(38) Mucalo, M. R.; Yokogawa, Y.; Toriyama, M.; Suzuki, T.; Kawamoto, Y.; Nagata, F.; Nishizawa, K. *J. Mater. Sci.: Mater. Med.* **1995**, *6*, 597−605.
(39) Mucalo, M. R.; Yokogawa, Y.; Suzuki, T.; Kawamoto, Y.; Nagata, F.; Nishizawa, K. *J. Mater. Sci.: Mater. Med.* **1995**, *6*, 658−669.
(40) Li, S.; Liu, Q.; de Wijn, J.; Wolke, J.; Zhou, B.; de Groot, K. *J. Mater. Sci.: Mater. Med*. **1997**, *8*, 543−549.
(41) Li, S. H.; Liu, Q.; de Wijn, J. R.; Zhou, B. L.; de Groot, K. *Biomaterials* **1996**, *18*, 389−395.
(42) Yokogawa, Y. *J. Mater. Sci.: Mater. Med.* **1997**, *8*, 407−412.
(43) Swart, J. G. N.; Driessen, A. A.; DeVisser, A. C. In *Hydrogels for Medical and Related Applications*; ACS Symposium Series; Andrade, J. D., Ed.; American Chemical Society: Washington DC, 1976; Vol. 31, pp 151−161.
(44) Mayer, J.; Schlam, R.; Featherstone, J. D. B. *J. Inorg. Biochem.* **1997**, *66*, 1−6.
(45) Fowler, B. O.; Moreno, E. C.; Brown, W. E. *Arch. Oral Biol*. **1966**, *11*, 477−492.
(46) Zhang, L. J.; Liu, H. G.; Feng, X. S.; Zhang, R. J.; Zhang, L.; Mu, Y. D.; Hao, J. C.; Qian, D. J.; Lou, Y. F. *Langmuir* **2004**, *20*, 2243−2249.
(47) Uchida, M.; Kim, H. M.; Kokubo, T.; Miyaji, F.; Nakamura, T. *J. Am. Ceram. Soc.* **2001**, *84*, 2041−2044.
(48) Kokubo, T. *Biomaterials* **1991**, *12*, 155−163.
(49) Lin-Vien, D.; Colthup, N. B.; Fateley, W. G.; Grasselli, J. G. *The Handbook of Infrared and Raman characteristic Frequencies of Organic Molecules*; Academic Press: London, 1991.
(50) Tanahashi, M.; Matsuda, T. *J. Biomed. Mater. Res.* **1997**, *34*, 305−315.

BM060583Q